Proceedings of the 2006 IEEE International Conference on Robotics and Automation
Orlando, Florida - May 2006

Bilateral Control of a Teleoperator for Soft Tissue Palpation: Design and Experiments

M. Tavakoli, R.V. Patel and M. Moallem

Canadian Surgical Technologies & Advanced Robotics (CSTAR) and
Department of Electrical and Computer Engineering
University of Western Ontario, London, ON N6A 5B9, Canada
tavakoli@uwo.ca, rajni@eng.uwo.ca, mmoallem@engga.uwo.ca

***Abstract*— In robot-assisted interventions, providing a surgeon with haptic information regarding contacts made between surgical instruments and tissue can improve task performance and reliability. In this paper, a force-reflective user interface is used with a sensorized surgical instrument to form a master-slave test-bed for studying haptic interaction in a soft-tissue endoscopic surgery environment. After modeling and parametric identification of the the master and the slave, bilateral controllers are designed and teleoperation experiments involving a single degree of freedom surgical task on soft tissue (palpation) are conducted. The transparency of the teleoperator in terms of transmitting the critical task-related information to the user in the context of soft-tissue surgical applications is investigated.**

I. Introduction

In addition to stability, transparency is the major performance requirement in the design of master-slave teleoperation systems. Transparency is defined as a correspondence between the master and slave positions and contact forces [1], or a match between the impedance perceived by the operator and the environment impedance experienced by the slave [2]. Transparency of a bilaterally controlled teleoperator depends on how well the slave-environment interaction forces are reflected to the user's hand by the master.

Studies on the effect of force reflection on various object manipulation and target acquisition tasks have shown that it improves the performance and efficiency of teleoperation by reducing the contact force levels, the sum of squared forces which is proportional to the energy consumption, the task completion time, and the number of errors [3], [4], [5]. Similarly, the precision, speed and force metrics are impacted by haptic feedback during surgical teleoperation. Research has been done to evaluate the effect of haptic perception on human sensory and motor behavior for a few surgical tasks. Study of the effect of force feedback on performing blunt dissection has shown that it can reduce the number of errors, the task completion time, and the contact forces [6]. The ability to sense the puncturing of different tissue layers during the needle insertion task improves when users receive haptic feedback [7]. On the other hand, the lack of feedback regarding instrument/tissue interactions for the surgeon can cause complications such as accidental puncturing of blood vessels or tissue damage [8], [9]. Indeed, lack of haptic feedback is regarded as a safety concern in endoscopic surgery because it would be potentially dangerous if instruments leave the limited field of view of the endoscopic camera. Furthermore, the endoscopic view, which can easily deteriorate due to fluids from the patient's body clouding the camera lens, can make it difficult to detect any tissue damage in the absence of haptic sensation for the surgeon.

This research was supported by the Ontario Research and Development Challenge Fund under grant 00-May-0709, infrastructure grants from the Canada Foundation for Innovation awarded to the London Health Sciences Centre (CSTAR) and the University of Western Ontario, the Natural Sciences and Engineering Research Council (NSERC) of Canada under grants RGPIN-1345 and RGPIN-227612, and the Institute for Robotics and Intelligent Systems under a CSA-IRIS grant.

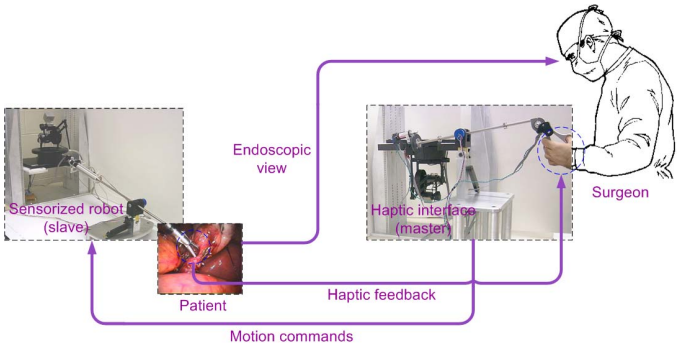

Fig. 1. Force-reflective master-slave surgical teleoperation.

Palpation is a procedure frequently used by surgeons to estimate tissue characteristics and greatly depends on haptic sensation. Indeed, haptic feedback can provide surgeons with the ability to distinguish between tissues with different stiffnesses when probing them robotically. Therefore, during robot-assisted palpation, it is imperative that the master-slave system acts transparently in terms of transmitting to the user the contact force versus deflection characteristics of the tissue. In this paper, bilateral controllers are designed for a master-slave test-bed developed for studying haptic feedback during endoscopic surgery. Experiments are conducted to evaluate the performance of the teleoperator in terms of accurate transmission of task-related information that is critical in the context of soft-tissue palpation.

This paper is organized as follow. Section II presents a brief overview of the master-slave test-bed for studying haptic feedback during endoscopic surgery, which encompasses a haptic user interface and a properly sensorized surgical instrument. In Section III, the dynamics of the master and the slave are determined. In Section IV, a general master-slave control formalism for position tracking and force reflection is described that makes use of position and force information at the master and the slave. This section also discusses how a system state observer can be used to estimate the operator's hand forces when the master does not have force/torque sensors, and how the transparency of the master-slave system can be evaluated with an emphasis on soft tissue applications. In Section V, the transparency of the master-slave system for different controllers is experimentally evaluated and discussed. Section VI has the concluding remarks.

II. Experimental Setup

A force-reflective master-slave system appropriate for use as an endoscopic surgery test-bed has been developed (Figure 1). Through the master interface, a user controls the motion of the slave arm (surgical tool) and receives force/torque feedback of the slave-environment interactions. This master-slave system

is a useful test-bed for investigating the performance and effectiveness of different bilateral control schemes for soft-tissue applications. The system can be tested under different circumstances in which it is expected to operate, for example, with varying tissue properties. The master and slave subsystems are briefly described next.

A. Force-reflective user interface

The developed haptic user interface that acts as the master is capable of providing the user with force sensation and kinesthetic sensation of the elasticity of an object in all five DOFs available in endoscopic surgery (pitch, yaw, roll, insertion, and handle open/close) [10]. A PHANToM 1.5A, which provides haptic feedback in three translational DOFs, is integrated into the user interface. A rigid shaft similar to an endoscopic instrument is passed through a fulcrum and attached to the PHANToM's endpoint, causing the motions of the handles grasped by the surgeon to be similar to those in endoscopic manipulation. Since the pitch, yaw and insertion motions of the instrument span the 3D Cartesian workspace of the PHANToM, force reflection is provided by the PHANToM in these three directions in the endoscopic instrument workspace. Additional mechanisms for force reflection in the roll and gripping directions are incorporated into the interface.

B. Sensorized surgical tool

The developed slave's surgical tool is an endoscopic instrument that serves as a robotic end-effector and is capable of actuating the open/close motions of a tip and rotations about its main axis [10]. The instrument is properly sensorized to measure its interactions with tissue in the form of forces or torques in all five DOFs present in endoscopic operations. Due to the problems posed by the incision size constraint in minimally invasive surgery, strain gauge sensors are integrated into the end effector to provide a non-invasive, efficient way of measuring interactions with tissue.

III. Dynamic Modeling

In this paper, the master and slave subsystems are tailored for force-reflective teleoperation in the twist direction only (i.e. rotations about the instrument axis). Therefore, the 1-DOF dynamic models of the master and the slave in the twist direction need to be determined in order to be able to implement the bilateral control laws discussed later. The dynamics of the 1-DOF master device excluding friction terms can be written as

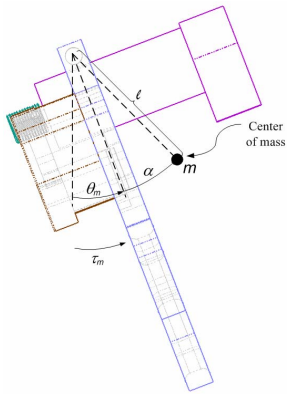

Fig. 2. The master handle.

$$\tau_m = (m\ell^2 + I_{zz})\ddot{\theta}_m + mg\ell\sin(\theta_m + \alpha) \qquad (1)$$

where, as shown in Figure 2, τ_m and θ_m are the joint torque and angular position at the motor output shaft, respectively. The center of mass m of the master is located at a distance ℓ and an angle α with respect to the master's axis of rotation. I_{zz} is the master's mass moment of inertia with respect to the axis of rotation.

To include the effect of friction in (1), consider two rigid bodies that make contact through elastic bristles. The friction force/torque τ_{fric} between the two can be modeled based on their relative velocity $\dot{\theta}$ and the bristles's average deflection z as [11], [12]:

$$\frac{dz}{dt} = \dot{\theta} - \sigma_0 \frac{|\dot{\theta}|}{s(\dot{\theta})} z \qquad (2)$$

$$\tau_{\text{fric}} = \sigma_0 z + \sigma_1 \frac{dz}{dt} + \sigma\dot{\theta} \qquad (3)$$

where σ_0, σ_1 are stiffness and damping parameters for the friction dynamics, and the term $\sigma\dot{\theta}$ accounts for viscous friction. A model of $s(\dot{\theta})$ that describes the Stribeck effect is given by:

$$s(\dot{\theta}) = \tau_c(1 - e^{-a|\dot{\theta}|}) + \tau_s e^{-a|\dot{\theta}|}$$

where τ_c and τ_s are Coulomb and stiction frictions, respectively. At steady state ($\frac{dz}{dt} = 0$), it follows from (2) that z approaches

$$z_{ss} = \frac{s(\dot{\theta})}{\sigma_0}\text{sgn}(\dot{\theta}).$$

Therefore, using (3), friction can be written as

$$\tau_{\text{fric}} = \sigma\dot{\theta} + \tau_c(1 - e^{-a|\dot{\theta}|})\text{sgn}(\dot{\theta}) + \tau_s e^{-a|\dot{\theta}|}\text{sgn}(\dot{\theta})$$

For the master device, assuming asymmetry in Stribeck friction effects when the master moves in the positive and negative directions, the dynamics can be written as

$$\begin{aligned}\tau_m &= M_m\ddot{\theta}_m + G\sin(\theta_m + \alpha) + \sigma\dot{\theta}_m \\ &+ \tau_{c_1}(1 - e^{-a_1|\dot{\theta}_m|})u_{\dot{\theta}_m} + \tau_{s_1}e^{-a_1|\dot{\theta}_m|}u_{\dot{\theta}_m} \\ &+ \tau_{c_2}(1 - e^{-a_2|\dot{\theta}_m|})u_{-\dot{\theta}_m} + \tau_{s_2}e^{-a_2|\dot{\theta}_m|}u_{-\dot{\theta}_m} \qquad (4)\end{aligned}$$

where τ_{c_i}, τ_{s_i} and a_i correspond to the positive direction ($\dot{\theta}_m > 0$) for $i = 1$ and to the negative direction ($\dot{\theta}_m < 0$) for $i = 2$, and $u(.)$ is the step function:

$$u_x = \begin{cases} 1, & x > 0 \\ 0, & x < 0 \end{cases}$$

A. Identification of the master dynamics

The master dynamics (4) are unknown in terms of rigid-body parameters for inertia and gravity M_m, G, α and in friction parameters σ, τ_{c_1}, τ_{s_1}, a_1, τ_{c_2}, τ_{s_2} and a_2. To identify these parameters, sinusoidal input torques $\tau_m = A\sin(2\pi ft)$ were provided to the master while the magnitudes and frequencies were chosen to cover various operating conditions of the system: $A \in \{0.03, 0.06, 0.09, 0.12, 0.15\}$ N.m and $f \in \{0.1, 0.5, 1\}$ Hz. Moreover, experiments were performed with the summation of two sinusoid signals as the input torque in order to increase the degree of persistence excitation of the input (the sum of n sinusoids is persistent excitation of an order no less than $2n - 2$ [13]). The resulting (τ_m, θ_m) pairs for all experiment were concatenated to form a complete set of input/output data. The joint position data were filtered by a 3^{rd}-order Butterworth filter implemented using a zero-phase-distortion routine (Matlab function *filtfilt*) to remove the measurement noise. To find $\dot{\theta}_m$ for offline system identification, the filtered position data were differentiated using the two-

TABLE I
IDENTIFIED MASTER MODEL PARAMETERS.

M_m	5.97×10^{-4}	kg.m^2
G	1.04×10^{-1}	N.m
α	9.3965	deg
σ	6.88×10^{-4}	N.m.sec/rad
τ_{c_1}	1.98×10^{-2}	N.m
τ_{s_1}	0	N.m
a_1	55.2	sec/rad
τ_{c_2}	-1.62×10^{-2}	N.m
τ_{s_2}	0	N.m
a_2	42.1	sec/rad

point central difference formula

$$\dot{y}(t) = \frac{y(t+T_s) - y(t-T_s)}{2T_s}$$

where T_s is the sampling time. Using the joint torque, position, velocity and acceleration data obtained above, a nonlinear multivariable minimization procedure (Matlab function *fminimax*) was used to find the parameter estimates that best fit the dynamic model (4). The identified parameters are listed in Table I. The above identified parameters were used to compensate for the gravity and friction effects, thus simplifying the dynamic model of the master to $\tau_m = M_m\ddot{\theta}_m$.

Using a method similar to the one described above, the slave's simplified model was experimentally determined to be $\tau_s = 9.8 \times 10^{-3}\ddot{\theta}_s$.

IV. MASTER-SLAVE BILATERAL CONTROL

In force-reflective master-slave teleoperation, a user operates from and receives feedback of slave/environment interactions via a master interface while a slave robot mimics the user's hand maneuvers on the remote environment. Taking into account the hand/master and the slave/environment interactions, the dynamics of the master and the slave can be written as:

$$\tau_m + \tau_h = M_m\ddot{\theta}_m \quad (5)$$
$$\tau_s - \tau_e = M_s\ddot{\theta}_s \quad (6)$$

where M_m and M_s are the master and the slave inertias, respectively. Moreover, θ_m, θ_s, τ_h, τ_e, τ_m and τ_s are the master and the slave positions, the torque (or force) applied by the user's hand on the master, the torque (or force) applied by the slave on the environment, and the control signals (torque or force) for the master and for the slave, respectively. The goal is to generate appropriate control signals τ_m and τ_s such that, regardless of the operator and environment dynamics, there is correspondence between measured positions and measured interactions at the master and the slave:

$$\theta_m = \theta_s$$
$$\tau_h = \tau_e \quad (7)$$

Consider the following general framework for bilateral control [1]:

$$\tau_m = M_m u_m - k_m\frac{\tau_e - \tau_h}{2} - \frac{\tau_e + \tau_h}{2}$$
$$\tau_s = M_s u_s - k_s\frac{\tau_e - \tau_h}{2} + \frac{\tau_e + \tau_h}{2} \quad (8)$$

where k_m and k_s are nonnegative constants and u_m and u_s will be found. Substituting (8) in (5) and (6) gives the closed-loop dynamics of the master and the slave as

$$\ddot{\theta}_m = u_m - M_m^{-1}(k_m+1)\frac{\tau_e - \tau_h}{2}$$
$$\ddot{\theta}_s = u_s - M_s^{-1}(k_s+1)\frac{\tau_e - \tau_h}{2} \quad (9)$$

The control requirements for transparent teleoperation (7) can be slightly eased by demanding asymptotic convergence of the position error $e_\theta = \theta_m - \theta_s$ to zero in addition to an exactly zero interaction error $e_\tau = \tau_h - \tau_e$:

$$\ddot{e}_\theta + k_v\dot{e}_\theta + k_p e_\theta = 0$$
$$e_\tau = 0 \quad (10)$$

Solving (10) and (9) together gives u_m and u_s, which after substitution in (8), give the following bilateral control laws:

$$\tau_m = M_m[\ddot{\tilde{\theta}} + k_v(\dot{\tilde{\theta}} - \dot{\theta}_m) + k_p(\tilde{\theta} - \theta_m)] - k_m(\tilde{\tau} - \tau_h) - \tilde{\tau} \quad (11)$$

$$\tau_s = M_s[\ddot{\tilde{\theta}} + k_v(\dot{\tilde{\theta}} - \dot{\theta}_s) + k_p(\tilde{\theta} - \theta_s)] - k_s(\tilde{\tau} - \tau_e) + \tilde{\tau} \quad (12)$$

Qualitatively, the above control laws try to make θ_m and θ_s track the desired trajectory $\tilde{\theta} = (\theta_m + \theta_s)/2$, and try to regulate τ_h and τ_e at the desired interaction $\tilde{\tau} = (\tau_h + \tau_e)/2$.

A. Observation of hand forces

The bilateral control laws (11) and (12) require the measurements of hand/master interactions τ_h and slave/environment interactions τ_e. In our master-slave system, while the slave's end-effector is sensorized to directly measure τ_e, we need to use the dynamic model of the master to estimate τ_h using a state observer. For this purpose, let's write the master dynamics $\tau_m + \tau_h = M_m\ddot{\theta}_m$, in which τ_m and τ_h are the contributions of the controller and the operator's force to the total joint torque respectively, in state-space form by choosing $x_1 = \theta_m$ and $x_2 = \dot{\theta}_m$:

$$\dot{x}_1 = x_2$$
$$\dot{x}_2 = {M_m}^{-1}(\tau_m + \tau_h)$$

To estimate the hand torques τ_h (and the joint velocity $\dot{\theta}_m$), the Nicosia observer can be used [14], [15]:

$$\dot{\hat{x}}_1 = \hat{x}_2 + k_2 e$$
$$\dot{\hat{x}}_2 = {M_m}^{-1}(\tau_m + k_1 e)$$
$$e = x_1 - \hat{x}_1 \quad (13)$$

where k_1 and k_2 are positive constants. As shown in Figure 3, the observer uses joint position and the portion of the joint torque that comes from the controller to find the externally

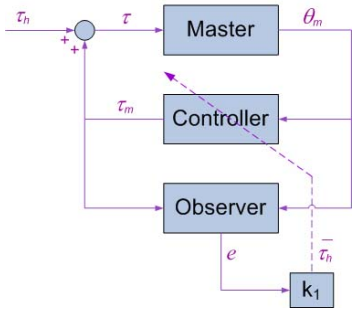

Fig. 3. Observer for estimating externally applied torques.

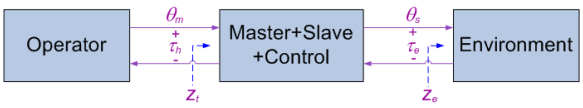

Fig. 4. Two-port network model of a master-slave teleoperator.

applied joint torque. It can be shown that the observer is asymptotically stable and the error equation is:

$$M\ddot{e} + k_2 M\dot{e} + k_1 e = \tau_h \tag{14}$$

In steady state, $\ddot{e} = \dot{e} = 0$. Therefore, the hand torque is estimated at low frequencies as $\overline{\tau}_h = k_1 e$.

B. Evaluation of transparency

To evaluate the transparency of teleoperation, the two-port network model of a master-slave system [16] as shown in Figure 4 is considered. In this framework, the master-slave system is described by

$$\begin{pmatrix} \tau_h \\ -\theta_s \end{pmatrix} = \begin{pmatrix} h_{11} & h_{12} \\ h_{21} & h_{22} \end{pmatrix} \begin{pmatrix} \theta_m \\ \tau_e \end{pmatrix}$$

For ideal master/slave position and force tracking as characterized by (7), we must have

$$\begin{aligned} h_{11} &= h_{22} = 0 \\ h_{12} &= -h_{21} = 1 \end{aligned} \tag{15}$$

Also, the operator will feel as if he/she is interacting directly with the environment (which is assumed to be passive) if the environment impedance $Z_e = \tau_e/\theta_s$ equals the impedance

$$Z_t = \frac{\tau_h}{\theta_m} = \frac{h_{11} + (h_{11}h_{22} - h_{12}h_{21})Z_e}{1 + h_{22}Z_e}$$

which is transmitted to the operator. The impedances will match ($Z_e = Z_t$) if (15) holds.

In evaluating transparency, a distinction needs to be made based on the environment impedance and the application of teleoperation. While hard-contact telerobotic applications (e.g. surface cleaning or bone milling) involve steady-state regulation of force, soft-tissue applications (e.g. probing tissue for determining tissue compliance) require dynamic position/force tracking and impedance matching. Indeed, it is during the probing process (transient mode) that position/force tracking and impedance matching are most required for correct detection of tissue compliance, rather than after the tissue is completely deformed (steady-state mode). Additionally, for soft-tissue surgical applications, it is very important for the teleoperation system to be able to transmit any change in the impedance of the environment to the operator [17]. For example, probing tissue for determining its compliance (called tissue palpation) depends greatly on the surgeon's ability to detect small changes in the tissue impedance. Therefore, as a measure of master-slave transparency for soft-tissue applications, the sensitivity of the transmitted impedance to changes in the environment impedance can be defined as

$$S_{z_t} = \left\| \frac{dZ_t}{dZ_e} \right\|_2 = \left\| \frac{-h_{12}h_{21}}{(1 + h_{22}Z_e)^2} \right\|_2$$

V. Palpation Experiments

In the 1-DOF master-slave system for performing palpation tests, the user manipulates the master causing the slave to probe the tissue via a small rigid beam attached to the endoscopic instrument. In our tests, the user first moves the master such that the slave considerably indents a soft object, and then moves the master back and forth for 20 seconds while the slave is still in contact with the object. The probing depth varies with the stiffness of the tissues used in the experiments. The slave interactions with the soft object are reflected to the user via the master interface. For the palpation tests, we use an object made of packaging foam material in addition to an artificial silicone-based tissue phantom (from the Chamberlain Group LLC., http://www.thecgroup.com) with higher stiffness compared to the foam material.

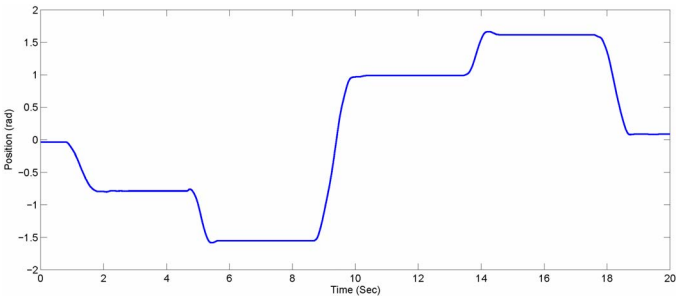

Fig. 5. Free-space profile of the master position.

As mentioned before, the gravity effects in the master interface have been compensated for such that the user does not feel any weight on his/her hand when the slave is not in contact with an object. This is important because in endoscopic operations and particularly during soft-tissue palpation, the weight of instruments hampers the accurate feeling of tissue properties by the surgeon. To examine the gravity compensation, with the slave end-effector in free space, the user rotated the master handle to several positions between -180° and +180° and released it. As shown in Figure 5, the master stays in the same position due to successful cancellation of gravity effects.

A. Selection of observer and controller gains

Using the dynamic model of the master and in the absence of a force sensor at the master, the observer (13) was used to estimate the hand torques τ_h. Using the observer's error dynamics (14), the gains k_1 and $k_2 = 2\sqrt{k_1/M_m}$ were chosen such that the observer has very fast poles at $(-350 \quad -350)$ with critical damping.

The two proportional-derivative controllers with gains k_p and k_v in (11) and (12), which wrap position control loops around the master and the slave, were used to place the master and slave closed-loop poles for fast responses. To this end, $(k_p \quad k_v) = (1600 \quad 80)$ were chosen. Noting that $\tilde{\theta} = (\theta_m + \theta_s)/2$ and $\tau_m = M_m\ddot{\theta}_m$ and $\tau_s = M_s\ddot{\theta}_s$ are the free-space dynamics, these gains result in the position error characteristic equation $\ddot{e}_\theta + 80\dot{e}_\theta + 1600e_\theta = 0$ for both the master and the slave, thus moving the closed-loop poles of the master and the slave to $(-40 \quad -40)$.

Given that $\tilde{\tau} = (\tau_h + \tau_e)/2$, the gain k_m determines the share of force feedback τ_e and local force feedback τ_h in the master control law (11). Similarly, k_s determines the share of force feedback τ_h and local force feedback τ_e in the slave control law (12). If $k_m = -1$ ($k_s = -1$), there will be no feedback of τ_e and full feedback of τ_h in the control law for the master (the slave). Also, if $k_m = 1$ ($k_s = 1$),

TABLE II

THE EFFECT OF GAINS k_m AND k_s ON BILATERAL CONTROL LAWS.

Cont.	k_m	k_s	Master e_θ	Master τ_h	Master τ_e	Slave e_θ	Slave τ_h	Slave τ_e	Chan. #	Architecture
a	-1	1	√	√	-	√	-	√	2	Pos–pos w/ master & slave local force feedback
b	-1	-1	√	√	-	√	√	-	3	Pos–(Pos+Force) w/ master local force feedback
c	1	1	√	-	√	√	-	√	3	(Pos+Force)–Pos w/ slave local force feedback
d	1	-1	√	-	√	√	√	-	4	(Pos+Force)–(Pos+Force) w/o local force feedback

there will be full feedback of τ_e and no feedback of τ_h in the control law for the master (the slave). Table II illustrates the control architectures that result from four combinations of the gains k_m and k_s. The number of communication channels shows how many position and force values are sent from the master to the slave and vice versa (excluding local feedback) in each bilateral control architecture. In the next section, the transparency of the master-slave system in transmitting task-related information to the user will be evaluated and compared for each of the above four controllers.

B. Experimental results

Two sets of experiments were done to find the hybrid parameters of the master-slave system. In the first test for each of the above four controllers, the user moves the master back and forth for 60 seconds while the slave is in free space. Since $\tau_e = 0$, the frequency responses $h_{11} = \tau_h/\theta_m$ and $h_{21} = -\theta_s/\theta_m$ can be found through spectral analysis (Matlab function *spa*). In the second test for each controller, the user moves the master back and forth for 60 seconds while the slave is in contact with a soft object (made of foam material). Using the knowledge of the frequency response estimates h_{11} and h_{21}, the other two hybrid parameters are derived as

$$h_{12} = \frac{\tau_h}{\tau_e} - h_{11}\frac{\theta_m}{\tau_e}$$

$$h_{22} = -\frac{\theta_s}{\tau_e} - h_{21}\frac{\theta_m}{\tau_e}$$

The hybrid parameters of the master-slave system for each controller are shown in Figure 6. The controllers *c* and *d* are closest to meeting the transparency requirements (15) while controllers *a* and *b* result in significant deviations of h_{12} from the ideal value of 1 (0 dB). Also, for controllers *c* and *d*, the transmitted impedances are closest to the average environment impedance and are most sensitive to the changes in the environment impedance (Figure 7).

The reason for the lack of transparency with the controllers *a* and *b* is the master local force feedback, which locally compensates for the user's hand forces. Indeed, for soft-tissue applications, local force feedback at the master amounts to the user feeling almost no force when the slave/environment interactions are small but nonzero. The use of local force feedback at the master is justifiable only in cases where the user cannot physically overcome the interactions between the slave and the environment, for instance when the slave and the environment have very high inertia and stiffness.

Similarities in the performance of controllers *c* and *d* in Figures 6 and 7 confirm the previous results [18] that local force feedback at the slave can eliminate the need for measuring or estimating the interactions between the hand and the master (τ_h) without degrading the performance. In fact, the performance is even better with controller *c* compared

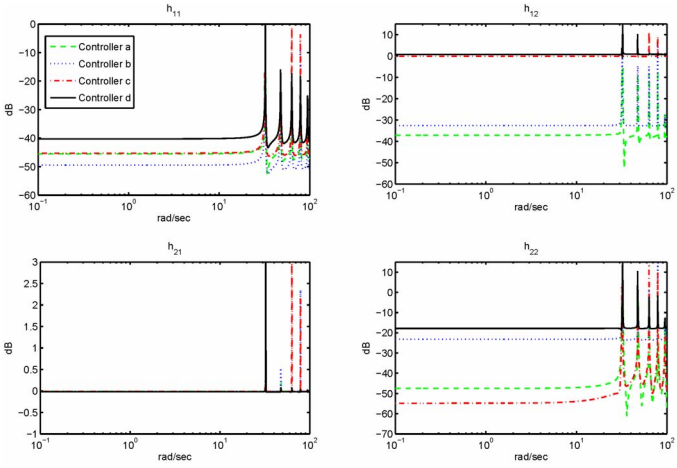

Fig. 6. The master-slave system hybrid parameters for four controllers.

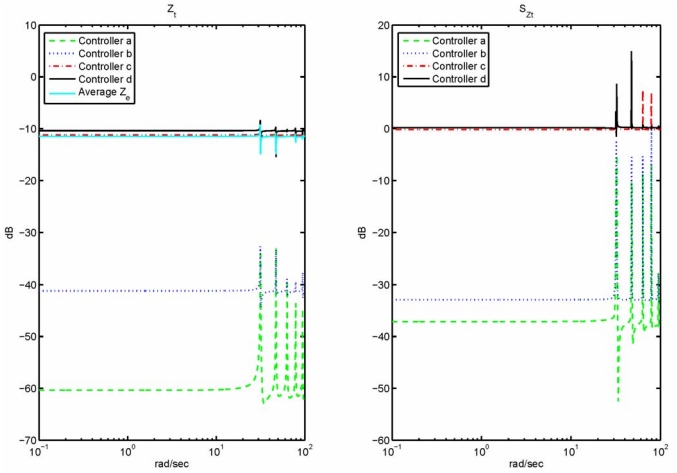

Fig. 7. The transmitted impedances and the average environment impedance (left), and the sensitivity of the transmitted impedances to changes in the environment impedance (right).

to *d*, which can be attributed to the local compensation for the slave/environment interactions. Therefore, in the presence of full slave local force feedback (controller *c*), the number of communication channels can be reduced from 4 to 3 (as τ_h is no longer needed for the control of the slave) without degrading transparency.

For controller *c* and when the slave makes contact with the foam object, the positions and interaction torques at the master and the slave sides are shown in Figure 8. As it can be seen, the slave closely follows the hand position and exerts a force on the object that matches the force applied by the hand on the master. Therefore, the user is successfully provided with an accurate perception of the compliance of the soft object. For the same controller with the foam object and with the

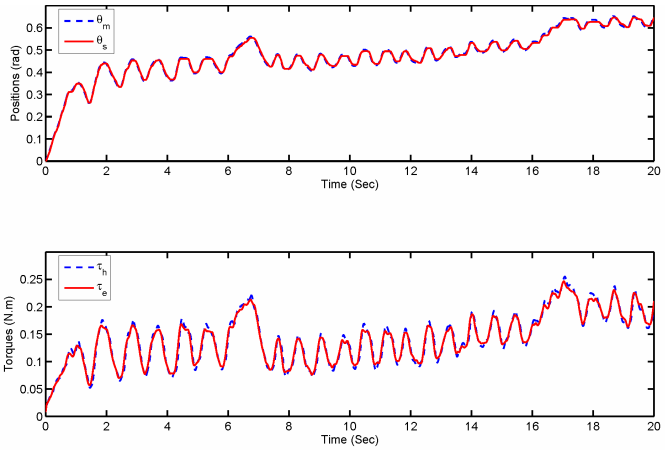

Fig. 8. Position and torque tracking with controller c for a soft environment.

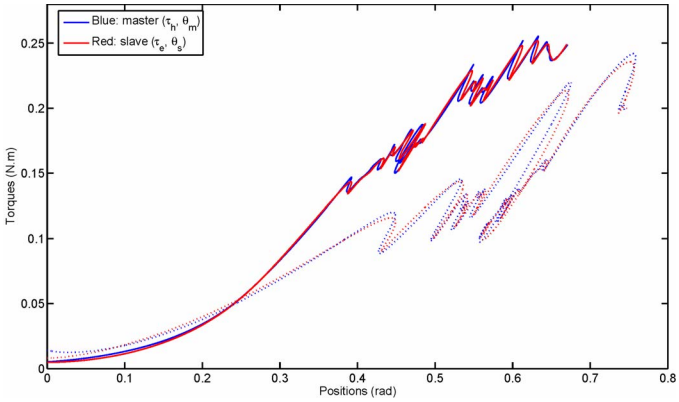

Fig. 9. Contact-mode profile of the torque-position relationship measured at the slave and as perceived by the user when controller c is used; solid: the silicone-based phantom, dotted: the foam object.

silicone-based object, the contact torques and deformations as measured at the slave (τ_e, θ_s) and as perceived by the user (τ_h, θ_m) are plotted versus each other (Figure 9). Since for each object these graphs are quite close, the master-slave system is acting transparently in terms of transmitting to the user the contact force/torque versus deflection characteristics of a tissue which are critical to the tissue palpation task. Users who tried the system were able to distinguish between tissues with different stiffnesses when probing them robotically.

VI. Concluding Remarks

In this paper, a haptic interface was used with a sensorized surgical instrument to set up a master-slave system for studying haptic interaction in an endoscopic surgery environment. Since the haptic interface (master) is not equipped with a force/torque sensor, a state observer based on the identified dynamical model of the master was utilized to estimate the force exerted by the operator's hand. A general bilateral control law was described that makes use of force and position information both at the master and the slave, and guarantees matching of forces and asymptotic convergence of positions. To measure the transparency of the master-slave system, a distinction needs to be made based on the nature of the slave/environment contacts; for soft contact applications, the teleoperator is required to demonstrate high sensitivity to changes in the environment impedance. As an example of soft-tissue surgical tasks, tissue palpation was considered. For this task, the transparency of the master-slave system for different control architectures was experimentally evaluated and compared. It was shown that for soft-tissue applications, while local force feedback at the master has a negative effect on transparency, local force feedback at the slave improves it. In addition, slave local force feedback eliminates the need for hand/master interaction information without degrading transparency. Evaluating the performance of human subjects [19] in terms of compliance discrimination under different teleoperator control schemes remains for future.

References

[1] Y. Yokokohji and T. Yoshikawa, "Bilateral control of master-slave manipulators for ideal kinesthetic coupling," *IEEE Trans. Robotics & Automation*, vol. 10, pp. 605–620, October 1994.

[2] D. A. Lawrence, "Stability and transparency in bilateral teleoperation," *IEEE Trans. Robotics & Automation*, vol. 9, pp. 624–637, October 1993.

[3] K. B. Shimoga, "A survey of perceptual feedback issues in dextrous telemanipulation: Part I. Finger Force Feedback," in *Proc. IEEE Annual Virtual Reality Int. Symp*, Seattle, Washington, 1993.

[4] G. C. Burdea, *Force and Touch Feedback for Virtual Reality*. New York: John Wiley & Sons, 1996.

[5] B. Hannaford and L. Wood, "Performance evaluation of a 6 axis high fidelity generalized force reflecting teleoperator," in *Proceedings of JPL/NASA Conference on Space Telerobotics*, Pasadena, CA, 1989.

[6] C. Wagner, N. Stylopoulos, and R. Howe, "Force feedback in surgery: Analysis of blunt dissection," in *The 10th Symp. on Haptic Interfaces for Virtual Environment and Teleoperator Systems*, Orlando, 2002.

[7] O. Gerovichev, P. Marayong, and A. M. Okamura, "The effect of visual and haptic feedback on manual and teleoperated needle insertion," in *Proceedings of the Fifth International Conference on Medical Image Computing and Computer Assisted Intervention – Lecture Notes in Computer Science (Vol. 2488)*, T. Dohi and R. Kikinis, Eds., 2002, pp. 147–154.

[8] G. T. Sung and I. S. Gill, "Robotic laparoscopic surgery: a comparison of the da Vinci and Zeus systems," *Urology*, vol. 58, no. 6, pp. 893–898, 2001.

[9] M. Hashizume, M. Shimada, M. Tomikawa, Y. Ikeda, I. Takahashi, R. Abe, F. Koga, N. Gotoh, K. Konishi, S. Maehara, and K. Sugimachi, "Early experiences of endoscopic procedures in general surgery assisted by a computer-enhanced surgical system," *Surg Endosc*, vol. 16, no. 8, pp. 1187–1191, 2002.

[10] M. Tavakoli, R. Patel, and M. Moallem, "Design issues in a haptics-based master-slave system for minimally invasive surgery," in *Proceedings of the IEEE International Conference on Robotics and Automation*, New Orleans, LA, 2004, pp. 371–376.

[11] C. C. de Wit, H. Olsson, K. J. Astrm, , and P. Lischinsky, "A new model for control of systems with friction," *IEEE Transactions on Automatic Control*, vol. 40, no. 3, pp. 419–425, 1995.

[12] M. R. Kermani, R. V. Patel, and M. Moallem, "Case studies of friction identifcation in robotic manipulators," in *Proceedings of IEEE International Conference on Control Applications*, Toronto, Canada, August 2005.

[13] T. Soderstrom and P. Stoica, *System Identification*. Prentice Hall International Ltd, 1989.

[14] S. Nicosia and P. Tomei, "Robot control by using only joint position measurements," *IEEE Transactions on Automatic Control*, vol. 35, no. 9, pp. 1058–1061, 1990.

[15] P. J. Hacksel and S. E. Salcudean, "Estimation of environment forces and rigid-body velocities using observers," in *Proceedings of the IEEE International Conference on Robotics and Automation*, San Diego, CA, 1994, pp. 931–936.

[16] B. Hannaford, "A design framework for teleoperators with kinesthetic feedback," *IEEE Transactions on Robotics and Automation*, vol. 5, pp. 426–434, 1989.

[17] M. C. Cavusoglu, A. Sherman, and F. Tendick, "Design of bilateral teleoperation controllers for haptic exploration and telemanipulation of soft environments," *IEEE Transactions on Robotics and Automation*, vol. 18, no. 4, pp. 641–647, 2002.

[18] K. Hashtrudi-Zaad and S. E. Salcudean, "Transparency in time-delayed systems and the effect of local force feedback for transparency teleoperation," *IEEE Trans. Robotics & Automation*, vol. 18, pp. 108–114, February 2002.

[19] A. Kazi, "Operator performance in surgical telemanipulation," *Presence: Teleoperators & Virtual Environments*, vol. 10, no. 5, pp. 495–510, October 2001.